DEVELOPMENT AND DISEASE

Axial skeletal defects caused by mutation in the spondylocostal dysplasia/pudgy gene *Dll3* are associated with disruption of the segmentation clock within the presomitic mesoderm

Sally L. Dunwoodie[1,2,*], Melanie Clements[1], Duncan B. Sparrow[2], Xin Sa[3], Ronald A. Conlon[3] and Rosa S. P. Beddington[1]

[1]Division of Mammalian Development, National Institute for Medical Research, The Ridgeway, Mill Hill, London NW7 1AA, UK
[2]Developmental Biology Unit, The Victor Chang Cardiac Research Institute, 384 Victoria Street, Darlinghurst, NSW 2010, Australia
[3]Department of Genetics, Case Western Reserve University, and University Hospitals Cleveland, 10900 Euclid Avenue, Cleveland, OH 44106-4955, USA

*Author for correspondence (e-mail: s.dunwoodie@victorchang.unsw.edu.au)

This article is dedicated to Rosa Beddington (March 23, 1956 to May 18, 2001) an extraordinary embryologist and a great friend

SUMMARY

A loss-of-function mutation in the mouse delta-like3 (*Dll3*) gene has been generated following gene targeting, and results in severe axial skeletal defects. These defects, which consist of highly disorganised vertebrae and costal defects, are similar to those associated with the *Dll3*-dependent pudgy mutant in mouse and with spondylocostal dysplasia (MIM 277300) in humans. This study demonstrates that *Dll3^neo* and *Dll3^pu* are functionally equivalent alleles with respect to the skeletal dysplasia, and we suggest that the three human *DLL3* mutations associated with spondylocostal dysplasia are also functionally equivalent to the *Dll3^neo* null allele. Our phenotypic analysis of *Dll3^neo*/*Dll3^neo* mutants shows that the

developmental origins of the skeletal defects lie in delayed and irregular somite formation, which results in the perturbation of anteroposterior somite polarity. As the expression of *Lfng*, *Hes1*, *Hes5* and *Hey1* is disrupted in the presomitic mesoderm, we suggest that the somitic aberrations are founded in the disruption of the segmentation clock that intrinsically oscillates within presomitic mesoderm.

Key words: Notch signalling, Somite, Spondylocostal dysplasia, Pudgy, *Dll3*, Mouse

INTRODUCTION

Notch signalling is an evolutionarily conserved mechanism used by metazoans to control the specification of cell fates through local interactions between cells (Artavanis-Tsakonas et al., 1999). As ligand and receptor are membrane associated, signalling is triggered by direct interaction of adjacent cells. In general, the Notch receptor is widely distributed within a cell population, while the ligand is restricted to a subset of cells (Fleming et al., 1990; Heitzler and Simpson, 1991; Vassin et al., 1987; Wharton et al., 1985). While several proteins participate in transmitting and regulating Notch signalling, a group of elements are defined as the core of this signalling pathway: in *Drosophila*, Delta and Serrate are Notch ligands, the transcription factor Suppressor of Hairless [Su(H)] is the major downstream effector (Bailey and Posakony, 1995; Lecourtois and Schweisguth, 1995), and genes of the *Enhancer of Split [E(Spl)]* locus (also transcription factors) are the primary targets of the pathway (Egan et al., 1998; Greenwald,

1998). Mammalian homologues have been identified for each of these core components and include *Notch1*, *Notch2*, *Notch3* and *Notch4* (Lardelli et al., 1994; Uyttendaele et al., 1996; Weinmaster et al., 1991; Weinmaster et al., 1992); Delta-like1 (*Dll1*)*, Dll3* and *Dll4* (Bettenhausen et al., 1995; Dunwoodie et al., 1997; Shutter et al., 2000); Serrate homologues *Jag1* and *Jag2* (Lindsell et al., 1995; Shawber et al., 1996); Su(H) homologue RBPjK (Furukawa et al., 1992; Schweisguth and Posakony, 1992) and Hairy and Enhancer of Split homologues *Hes1*, *Hes5* (Sasai et al., 1992; Takebayashi et al., 1995), *Hey1* and *Hey2* (also known as *HRT/Hesr*) (Kokubo et al., 1999; Leimeister et al., 1999; Nakagawa et al., 1999).

The Notch signalling pathway is deployed in three types of processes: lateral inhibition, lineage decisions and boundary formation (Bray, 1998). In vertebrates, somite segmentation relies on boundary formation in rostral presomitic mesoderm, coincident with expression of genes associated with Notch signalling (del Barco Barrantes et al., 1999). Accordingly, boundary formation with respect to somitogenesis commands

considerable interest because, in mouse, core Notch signalling components (Notch1, Dll1, Dll3 and RBPjK) and signalling modifiers [lunatic fringe (Lfng) and presenilin 1] are required for normal somite formation and anterior-posterior somite polarity (Conlon et al., 1995; Evrard et al., 1998; Hrabe de Angelis et al., 1997; Kusumi et al., 1998; Oka et al., 1995; Swiatek et al., 1994; Wong et al., 1997; Zhang and Gridley, 1998). In zebrafish, a mutation in *deltaD* is responsible for the *after eight* mutant (which makes only the first eight somites), demonstrating that Notch signalling is also required in this species (Holley et al., 2000).

In presomitic mesoderm, Notch signalling activity is not restricted to boundary formation, but also appears to be required at earlier (albeit interrelated) stages during the development of presomitic mesoderm (Pourquie, 2000). Presomitic mesoderm acquires a prepattern that distinguishes rostral presomitic mesoderm from caudal, and rostrally this culminates in segmentation with anteroposterior polarity being established in a single presomite unit. The periodicity with which this prepattern develops is postulated to require a 'segmentation clock' that oscillates in accordance with the formation of each new somite (Cooke, 1998; Cooke and Zeeman, 1976). Genes have been identified in chick (*hairy-1*), mouse (*Lfng*, *Hes1*, *Hes7* and *Hey2*) and in zebrafish (*her1, deltaC* and *deltaD*) that produce transcripts that are seen to pass in a caudal to rostral direction (Aulehla and Johnson, 1999; Forsberg et al., 1998; Jiang et al., 2000, Bessho et al., 2001; Jouve et al., 2000; Leimeister et al., 2000; Leimeister et al., 1999; McGrew et al., 1998; Palmeirim et al., 1997). It is likely that Notch signalling is associated with the 'segmentation clock' because these genes are allied with Notch signalling: *Fringe* in *Drosophila* acts upstream of the pathway by modifying the response of Notch to ligand binding; *deltaC* and *deltaD* are ligands of Notch; and *Hairy* and *Enhancer of Split* homologues (*chairy-1, Hes1, Hes7* and *Hey2*) are likely or proven downstream target genes of Notch signalling (Bessho et al., 2001; de la Pompa et al., 1997; del Barco Barrantes et al., 1999; Fleming et al., 1997; Holley et al., 2000; Jouve et al., 2000; Klein and Arias, 1998; Leimeister et al., 2000; Leimeister et al., 1999; Ohtsuka et al., 1999; Panin et al., 1997). This oscillatory pattern of gene expression consists of rostral and caudal expression components within the presomitic mesoderm. Characteristically, the rostral domain is condensed and corresponds to a half-somite segment, while the caudal domain is broader and moves rostrally from the caudal presomitic mesoderm. In cases where the core components of Notch signalling have been targeted, null mutant embryos show disrupted oscillatory gene expression within the presomitic mesoderm. The most severe effects are seen in *Dll1* and *RBPjK* mutants, while milder expression perturbations have been reported for *Notch1* and the *Dll3pu* (pudgy) mutant allele (del Barco Barrantes et al., 1999; Jouve et al., 2000; Kusumi et al., 1998; Leimeister et al., 2000). This suggests that Notch signalling is required to propagate and maintain oscillation of the segmentation clock, probably through a feedback mechanism similar to that identified in *Drosophila* and nematode (de Celis and Bray, 1997; Huppert et al., 1997; Kimble and Simpson, 1997). However, studies in zebrafish by Jiang and colleagues propose that Notch signalling is not required to establish oscillation within the presomitic mesoderm but rather to keep the oscillations of neighbouring cells synchronised (Jiang et al., 2000).

To understand how presomitic mesoderm prepatterning and segmentation culminates in somite formation, the role of core components of Notch signalling needs to be examined. In mouse, three Notch ligands are expressed in presomitic mesoderm. While *Dll1* and jagged 1 (*Jag1*) expression is coincident in the posterior half of the forming somite, *Dll3* is expressed in the anterior half (del Barco Barrantes et al., 1999; Dunwoodie et al., 1997; Mitsiadis et al., 1997; Zhang and Gridley, 1998), leading to the juxtaposition of *Dll1/Jag1* co-expressing cells with *Dll3*-expressing cells across a forming somite boundary and within a forming somite. Genetic analysis reveals no somitic or vertebral defect in mouse *Jag1* null mutants; however, butterfly vertebrae do occur in Alagille Syndrome in which *JAG1* is mutated (Krantz et al., 1997). By contrast, in *Dll1* mutants the basic metameric unit within paraxial mesoderm is maintained albeit with a loss of anteroposterior polarity (del Barco Barrantes et al., 1999; Hrabe de Angelis et al., 1997; Xue et al., 1999). In the case of *Dll3*, pudgy mice have a highly disorganised vertebrocostal skeleton with delayed somite formation (Gruneberg, 1961; Kusumi et al., 1998). In humans, spondylocostal dysplasia (SCD) is characterised by similar vertebrocostal defects, and where SCD follows a recessive mode of inheritance, mutations have been reported in the *DLL3* gene (Bulman et al., 2000).

We report the phenotypic analysis of a loss-of-function mutation in mouse *Dll3* and demonstrate that this mutation affects the axial skeleton and components of the peripheral nervous system. The skeletal defects are severe and similar to those observed in cases of *DLL3*-dependent SCD in humans and *Dll3*/pudgy mice. In addition we show that the two mouse *Dll3* mutant alleles, *Dll3neo* and *Dll3pu*, are functionally equivalent with respect to the skeletal defects. We use the null *Dll3neo* allele to show that the skeletal defects originate in aberrant somite formation, which are probably due to an altered 'segmentation clock' in presomitic mesoderm.

MATERIALS AND METHODS

Targeting vector and generation of chimaeras

The *Dll3* genomic clone was isolated from a 129sv library (Stratagene). Genomic DNA (2.5 kb and 3.4 kb) was cloned either side of PGK1-neomycin (Fig. 1A). This vector was linearised with *Xho*I and electroporated into CGR8 embryonic stem (ES) cells as described (Harrison et al., 1995). After double selection with G418 and gancyclovir, 800 ES cell clones were picked, expanded and frozen according to standard methods (Hogan et al., 1994). Homologous recombinants were identified following *Bam*HI restriction and hybridisation with sequences located 5′ (Fig. 1A) and 3′ external to the recombination sites. Four targeted clones were identified and chimaeric males representing three clones were mated with C57BL6 females to establish F0 heterozygotes. These were crossed to C57BL6 mice and their progeny were intercrossed for phenotypic analysis. Results were pooled from the three distinct targeted *Dll3/Dll3neo* lines as individuals were phenotypically identical.

Genotyping *Dll3*, *Dll3Neo* and *Dll3pu* alleles

Genotyping was performed by PCR or Southern blot (Fig. 1B,C) (Hogan et al., 1994). PCR primers used to distinguish between *Dll3* and *Dll3neo* were D3F (5′-tatgcaagactccatcattgagcc-3′), D3R (5′-ccaatggaggagccttatccag-3′) and PGK1 (5′-atgctccagactgccttggg-3′). The *Dll3pu* allele was identified according to Kusumi et al. (1998).
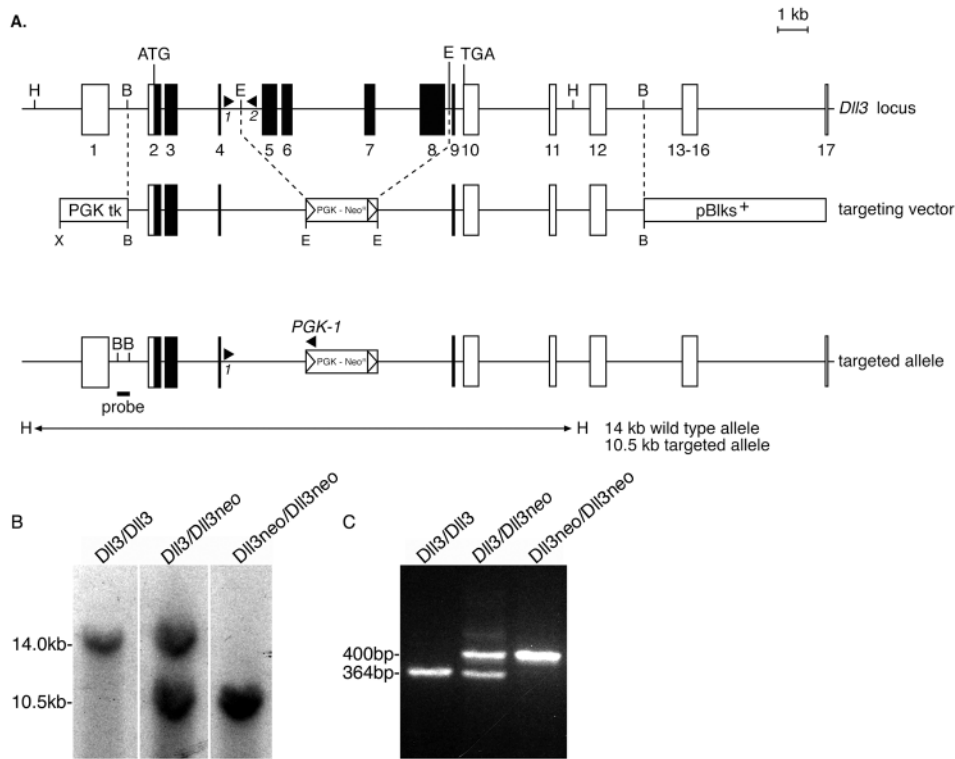
Fig. 1. Generation of *Dll3* null mutant mice. (A) Mouse *Dll3* locus, targeting vector and targeted allele, exons are boxed with coding exons in black. The neomycin resistance gene and the Herpes simplex virus thymidine kinase gene transcribed by the PGK1 promoter are shown (PGK-*Neo*, PGKtk). The genomic probe that identifies different *Hin*dIII fragment sizes for the wild type (14 kb) and targeted (10.5 kb) alleles is shown. PCR primers are defined by black arrowheads 1 (D3F) and 2 (D3R), and PGK-1. (B) Southern blot analysis of genomic DNA from wild-type (*Dll3/Dll3*), heterozygous (*Dll3/Dll3^{neo}*) and homozygous null (*Dll3^{neo}/Dll3^{neo}*) mice. (C) PCR genotyping of embryos and mice from heterozygous matings. Primers D3F, D3R and PGK1 amplified 340 bp and 450 bp representing the *Dll3* and *Dll3^{neo}* alleles, respectively.

Histology, in situ hybridisation and immunohistochemistry

For histology, embryos were fixed in Bouin's fixative, dehydrated, embedded in paraffin wax, sectioned and stained with Hematoxylin-Eosin as described (Kaufman, 1992). Whole-mount RNA in situ hybridisation was performed as described (Harrison et al., 1995). Probes for the following genes were used: *Dll3* (Dunwoodie et al., 1997), *Uncx4.1* (Mansouri et al., 1997), *Cer1* (Biben et al., 1998), *Hes1, Hes5* (Akazawa et al., 1992; Sasai et al., 1992), *Lfng* (Johnston et al., 1997) and *Mesp2* (Saga et al., 1997). pSPORT1-beta-spectrin2 (6412-8172bp) was linearised with *Sal*I and antisense RNA generated using SP6 RNA polymerase. Skeletal preparations were performed at 14.5 dpc according to Jegalian and De Robertis (Jegalian and De Robertis, 1992). Whole-mount immunohistochemistry with anti-neurofilament monoclonal antibody 2H3 (Developmental Studies Hybridoma Bank) was performed according to Mark et al. (Mark et al., 1993).

RESULTS

Targeted disruption of the *Dll3* gene and generation of null mutant mice

To engineer a *Dll3* null mutation a targeting vector was constructed deleting 5.4 kb of genomic sequence (Fig. 1A) including amino acids G135-S556 containing the DSL (Notch binding domain), all EGF repeats and the transmembrane domain (Dunwoodie et al., 1997; Kusumi et al., 1998). Mice heterozygous for the targeted allele (*Dll3^{neo}*) appeared normal. *Dll3* wild-type and targeted (*Dll3^{neo}*) alleles were distinguished by Southern blot or multiplex PCR analysis (Fig. 1B,C). Heterozygous (*Dll3/Dll3^{neo}*) intercrosses resulted in the birth of homozygous (*Dll3^{neo}/Dll3^{neo}*) null mice. Genotypic

analysis at post birthday (PBD) ten showed a deviation from the expected Mendelian ratio with 87% fewer *Dll3^{neo}/Dll3^{neo}* mutants present (Table 1). Further analysis indicated that *Dll3^{neo}/Dll3^{neo}* mutants were dying between birth and PBD10, as the genotype showed no deviation from the expected ratio during the prenatal period and at birth.

Skeletal defects in homozygous mutants

Dll3^{neo}/Dll3^{neo} mutants were easily identified because they had

Table 1. Genotypes of mice resulting from heterozygous intercrosses

| Stage | Genotype | | | P |
	Dll3/Dll3	*Dll3/Dll3^{neo}*	*Dll3^{neo}/Dll3^{neo}*	
Postnatal	366	544	84	0.000
Birth	58	120	36	0.021
Pre-natal	307	575	282	0.537
18.5 dpc	2	6	5	0.481
17.5 dpc	2	3	2	0.982
15.5 dpc	5	9	4	0.946
14.5 dpc	8	15	9	0.911
13.5 dpc	15	21	9	0.406
12.5 dpc	16	37	16	0.834
11.5 dpc	41	38	21	0.001
10.5 dpc	103	163	88	0.175
9.5 dpc	73	172	60	0.047
8.5 dpc	46	95	56	0.532
7.5 dpc	11	43	26	0.048

The genotype analysis combines data from three independent clones. Mice grouped into the postnatal category were between day 10 and day 20 at the time of tail biopsy. Ratios of genotypes were tested for goodness of fit to expected Mendelian segregation (1:2:1) by χ^2 analysis, calculated with two degrees of freedom. dpc, days post coitum.
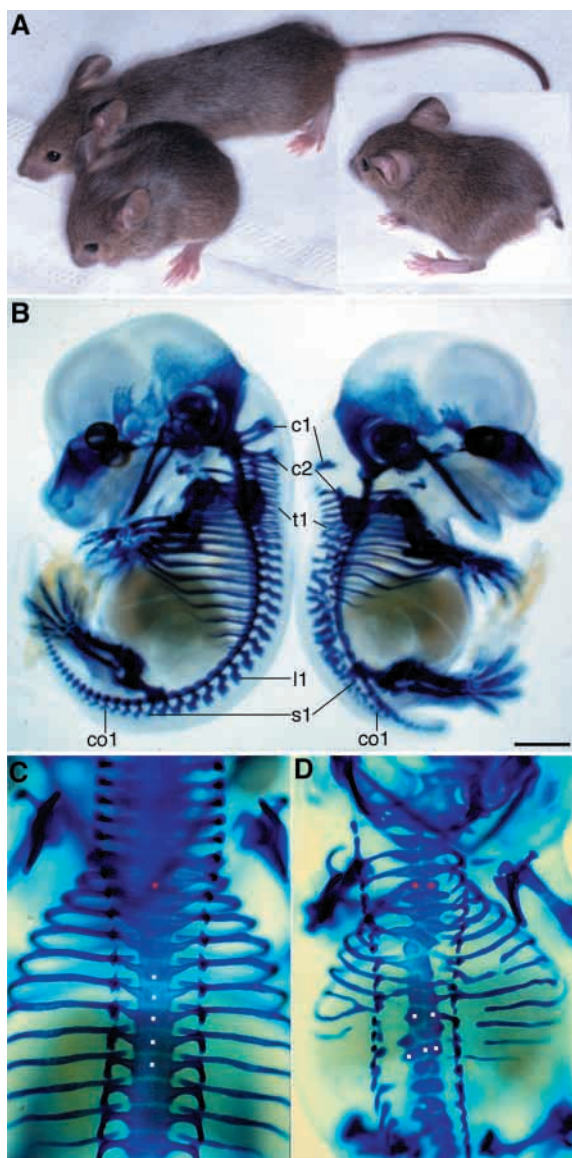
Fig. 2. *Dll3^neo^/Dll3^neo^* mutants have a truncated body axis and skeletal dysplasia. (A) *Dll3^neo^/Dll3^neo^* mutants have a shortened body and tail compared with *Dll3/Dll3^neo^* mice. (B) Lateral view of Alcian Blue-stained embryos (14.5 dpc). The positions of vertebrae: cervical (c1 and c2), thoracic (t1), lumbar (l1), sacral (s1) and coccygeal (co1) are indicated. (C,D) Dorsal view of developing skeleton. (C) *Dll3/Dll3^neo^* embryo from left in (B). (D) *Dll3^neo^/Dll3^neo^* embryo from right in B. Red dots indicate centrum corresponding to the position of t1, white dots indicate centrum of thoracic vertebrae. Note that in *Dll3^neo^/Dll3^neo^* embryos, ossification centres lie two and three in a row instead of lying in column as seen in *Dll3/Dll3^neo^* embryo (C). Scale bar: 1.35 mm in B; 675 μm in C.

a shortened body (40% reduced) and a short tail (Fig. 2A). This defect was completely penetrant and was apparent in preskeletal cartilage in embryos at 14.5 dpc (Fig. 2B). Skeletal disorganisation extended from the most rostral vertebra (cervical 1) along the length of the vertebral column. The vertebral arches were highly disorganised with ribs sometimes fused or absent (compare Fig. 2C with 2D). Shortening of the

body was probably due to fewer vertebrae, and single vertebra showed more than one centre of ossification. In addition, the short tail in *Dll3^neo^/Dll3^neo^* individuals was due to the absence of approximately 20 coccygeal vertebrae.

Histological analysis at 13.5 dpc demonstrated irregularities in the peripheral nervous system (Fig. 3). In *Dll3/Dll3^neo^* embryos, the cartilage primordia of the vertebrae were regularly spaced like the dorsal root ganglia (Fig. 3A-C), while these were disorganised in *Dll3^neo^/Dll3^neo^* embryos (Fig. 3D-F). The cartilage primordium of the bassioccipital bone appeared normal, with disorganisation apparent from the rostralmost vertebra (cervical 1) and extending along the entire length of the vertebral column (Fig. 2 and data not shown).

Neural crest cells arise without periodicity along the length of the neural tube; those that migrate ventrally condense to form ganglia (Larsen, 1997; Tosney, 1978; Weston, 1963). Similarly, axons of motoneurones that pass through a ventral root leave the neural tube along a broad front but they too condense to form discrete units. These ganglia and axons are located periodically along the length of the trunk despite the fact that they arise without periodicity from the neural tube. Periodicity is generated as the passage of neural crest and axons is restricted so that they migrate only through the anterior of the sclerotome (Stern and Keynes, 1987). This behaviour is not autonomous to the neural crest cells and axons, but rather is enforced by the sclerotome (Bronner Fraser, 1986; Rickmann et al., 1985; Teillet et al., 1987). Anti-neurofilament antibody confirmed the regular periodicity with which the spinal nerves and ganglia form in *Dll3/Dll3^neo^* embryos (Fig. 4A,B,F). Conversely, *Dll3^neo^/Dll3^neo^* embryos exhibited either lost or irregular periodic arrangement of ganglia and axons (Fig. 4C-E). In addition, the neural tube was often 'kinked' in *Dll3^neo^/Dll3^neo^* embryos (compare Fig. 4F with 4G).
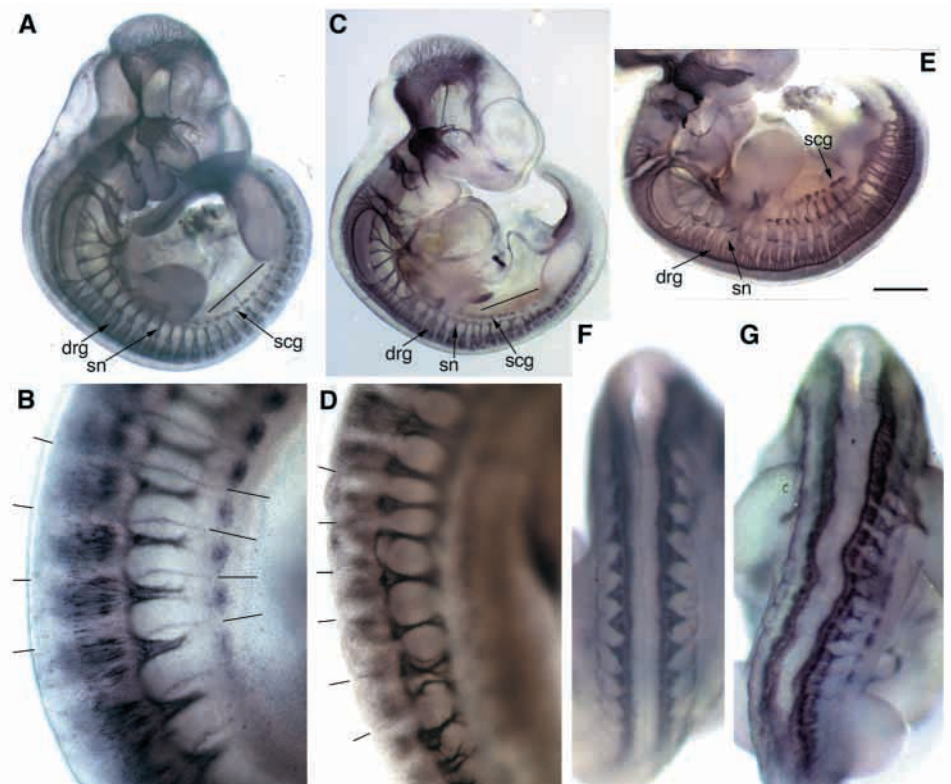
Somitogenesis is abnormal in *Dll3^neo^/Dll3^neo^* embryos

Epithelial somites form from mesenchymal presomitic mesoderm in a rostrocaudal manner such that cells at the rostralmost part of the presomitic mesoderm will be the next to undergo a mesenchymal to epithelial transition to form a somite. Accordingly, cells at the caudal aspect of the presomitic mesoderm have only recently been recruited from the primitive streak (or tail bud) and so will form a somite only once they are located at the rostralmost position of the presomitic mesoderm. Epithelial somites were formed in *Dll3^neo^/Dll3^neo^* embryos; however, somite formation was delayed and the degree of condensation was reduced (Fig. 5). Using morphological landmarks and *Mesp2* gene expression (Saga et al., 1997), the site of somite boundary formation was clearly identified in *Dll3/Dll3^neo^* embryos (Fig. 5A,B). In *Dll3^neo^/Dll3^neo^* embryos, the paraxial mesoderm was not organised into epithelial somites immediately rostral to this site (Fig. 5C-F). The extent of mesenchyme was inconstant, suggesting that the delay in somite formation was variable between embryos. The expression of *Mesp2* where the boundary should form in the *Dll3^neo^/Dll3^neo^* mutants demonstrates that this site is defined at the molecular level, despite the fact that a morphological transition was absent and that *Mesp2* expression is independent of *Dll3* function. Next, we examined whether somitogenesis was delayed from the
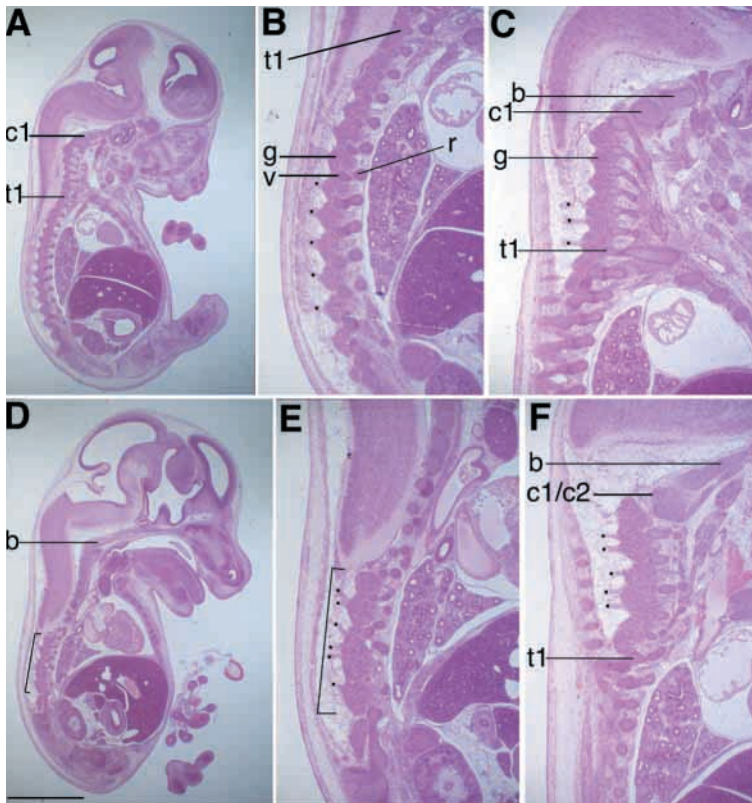
Fig. 3. Skeletal dysplasia in *Dll3^neo^/Dll3^neo^* mutants leads to disorganisation of the peripheral nervous system. Parasagittal sections of 13.5 dpc *Dll3/Dll3^neo^* (A-C) and *Dll3^neo^/Dll3^neo^* (D-F) embryos. (A) Dorsal root ganglia and cartilage primordia of vertebrae are evenly spaced along the axis. (B) Enlargement of thoracic region shown in A. (C) The cartilage primordium of the bassioccipital bone and the first two cervical vertebrae are clearly identifiable as is the rostralmost dorsal root ganglion which lies caudal to cervical vertebra 2. Note the even spacing of spinal nerves (dots) in (B,C). (D) Dorsal root ganglia are irregular in size and shape and are fused. This is evident in the thoracic region (E), where the arrangement of vertebrae and rib heads is also highly disorganised. Fused dorsal root ganglia are also evident in the cervical region (F) where the cartilage primordia of cervical vertebrae 1 and 2 are fused. Note the uneven distribution of spinal nerves (dots) in (E,F). Dorsal root ganglion (g), vertebra (v), head of rib (r), cervical vertebra (c), thoracic vertebra (t), basioccipital bone (b). Scale bar: 1.8 mm in A,D; 680 μm in B,C,E,F.

Fig. 4. Elements of the peripheral nervous system are disorganised in *Dll3^neo^/Dll3^neo^* mutants. Whole-mount immunohistochemistry with an anti-neurofilament antibody of *Dll3/Dll3^neo^* embryos (A,B,F) and *Dll3^neo^/Dll3^neo^* mutant embryos (C-E,G) at 10.5-11.5 dpc. Lateral view (A-E) and dorsal view (F,G). (A) Dorsal root ganglia (drg), spinal nerve (sn) and sensory chain ganglia (scg) are evenly spaced. (B) The region between the fore and hind limbs of (A) is marked with a line (anterior towards the top). Lines dorsal and ventral to the somites mark individual somitic segments and show that ventral spinal axons pass exclusively through the anterior of the somite segment. (C) dsg, sn and scg are unevenly spaced. (D) The region between the fore and hind limbs of (C) is marked with a line (anterior towards the top). Lines mark out individual somitic segments and show that the spinal axons pass through the anterior, posterior or central part of the somite segment. (E) *Dll3^neo^/Dll3^neo^* mutant embryo (11.5 dpc). The disarray of spinal axons and scg is more severe

than in (C). (F) Dorsal view of A shows a straight neural tube, while in G the same view of E indicates that the neural tube is 'kinked' (anterior towards the top). Scale bar: 730 μm in A,C,E; 150 μm in B,D; 365 μm in F,G.

Fig. 5. Somitogenesis is delayed and irregular with reduced mesenchymal condensation in *Dll3^neo^/Dll3^neo^* mutants. (A-F) Lateral view of the caudal part of 9.5 dpc embryos after RNA whole-mount in situ hybridisation with *Mesp2*. The black line (A-D) indicates the position of the last formed somite boundary and *Mesp2* expression lies just caudal to the somite boundary that is next to form in (A,B). (A) Regularly sized and spaced epthithelial somites are present in *Dll3/Dll3^neo^* embryos. The distance between the band of *Mesp2* expression and the last formed somite is equivalent to one somite width. (C) Irregularly sized epthithelial somites are formed in this *Dll3^neo^/Dll3^neo^* embryo. The distance between the band of *Mesp2* expression and the last formed somite is equivalent to three somite widths. (E) No epithelial somites were detected in this *Dll3^neo^/Dll3^neo^* embryo. The band of *Mesp2* expression is in an equivalent position to that in A. (B,D,F) Higher magnifications of A,C,E. (G-L) Ventral view of 8.5 dpc embryos after whole-mount in situ hybridisation with β-spectrin 2. The arrow indicates where the next somite boundary will form. (G,H) Epithelialisation of mesenchyme to form somites is evident and marked by distinct β-spectrin 2 gene expression in the centre of the somite in *Dll3/Dll3^neo^* embryos.

(I-L) Epithelialisation of mesenchyme is poor in *Dll3^neo^/Dll3^neo^* mutants, with diffuse β-spectrin 2 expression. (H,J,L) Higher magnifications of G,I,K. Scale bar: 200 μm in A,C,E; 100 μm in B,D,F; 160 μm in G,I,K; 80 μm in H,J,L.
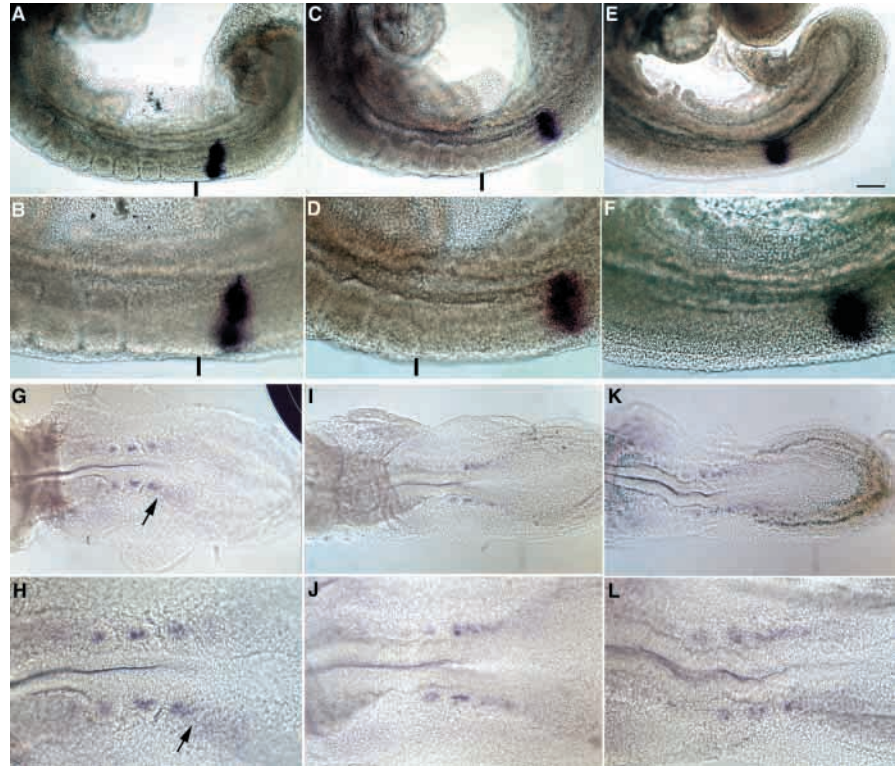
onset of somite formation. Physical boundaries were evident between somites in *Dll3/Dll3* and *Dll3/Dll3^neo^* embryos (Fig. 5G,H), but were not detected in *Dll3^neo^/Dll3^neo^* mutants (Fig. 5I-L). Although intersomitic boundaries were not observed metameric units were evident as reduced epithelialisation of paraxial mesoderm was detected by the less condensed expression of the cytoskeletal protein β-spectrin2. Notwithstanding the delay and irregularity associated with somite formation in *Dll3^neo^/Dll3^neo^* mutants, they differentiated into muscle, dermis and skeleton, indicating that dorsoventral pattern was established and cellular differentiation achieved (Fig. 3 and data not shown).

In order that the specified number of evenly sized somites are generated, a boundary must form at regular time intervals in the rostral presomitic mesoderm, and this most probably requires the dynamic action of Lfng in the presomitic mesoderm (Aulehla and Johnson, 1999; Forsberg et al., 1998; McGrew et al., 1998). *Lfng* transcripts are localised to one or two bands adjacent to the forming somite boundary in the rostral presomitic mesoderm, and in a caudal dynamic domain. A reiterative pattern is produced which is completed in approximately 2 hours in the mouse, roughly the period of time required to generate a somite (Goedbloed and Smits-van Prooije, 1986; Tam and Tan, 1992). Given that the somite boundary does not form at the usual site in *Dll3^neo^/Dll3^neo^* mutants, we examined *Lfng* expression. In *Dll3/Dll3* and *Dll3/Dll3^neo^* embryos, *Lfng* expression was detected in both rostral and caudal presomitic mesoderm (12/15) in patterns consistent with those reported in mouse (Aulehla and Johnson, 1999; Forsberg et al., 1998) (Fig. 6A). By contrast, a rostral

domain of expression was apparent in the absence of a caudally located expression domain in *Dll3^neo^/Dll3^neo^* mutants (10/10) (Fig. 6B).

Delayed and irregular somite formation could explain the skeletal dysplasia in *Dll3^neo^/Dll3^neo^* mutants. However, as each vertebra is derived from the anterior of one somite and the posterior of an adjacent somite (Bagnall et al., 1988; Bagnall et al., 1989; Huang et al., 1996; Stern and Keynes, 1987), vertebral development is also dependent upon anteroposterior somite identity being clearly defined. *Uncx4.1* expression marks the posterior nascent somite and later, the posterior lateral sclerotome (Fig. 6C) (Mansouri et al., 1997; Neidhardt, 1997) and was used to examine somite polarity. Expression in posterior epithelial somites was clearly evident in caudal somites dissected from *Dll3/Dll3^neo^* embryos (Fig. 6F). By contrast, *Uncx4.1* was mostly (5/8) expressed in a continuous domain in the paraxial mesoderm of *Dll3^neo^/Dll3^neo^* embryos, the remainder (3/8) showing periodic, but not exclusively posterior, expression (Fig. 6D,E). In addition, epithelial somites were not discernable in paraxial mesoderm dissected from *Dll3^neo^/Dll3^neo^* mutants (compare Fig. 6F with 6G). As paraxial mesoderm of *Dll3^neo^/Dll3^neo^* embryos displays posterior character (albeit disorganised), we examined whether anterior character was apparent. Mouse *Cer1* was expressed in stripes in the anterior presomitic mesoderm and the anterior of nascent somites in *Dll3/Dll3* (12/12) and *Dll3/Dll3^neo^* (25/25) embryos (Biben et al., 1998; Fig. 6H). *Dll3^neo^/Dll3^neo^* mutants also expressed *Cer1* in paraxial mesoderm, demonstrating the presence of anterior character; however, as for *Uncx4.1*, expression lacked periodicity (11/11; Fig. 6I-K).
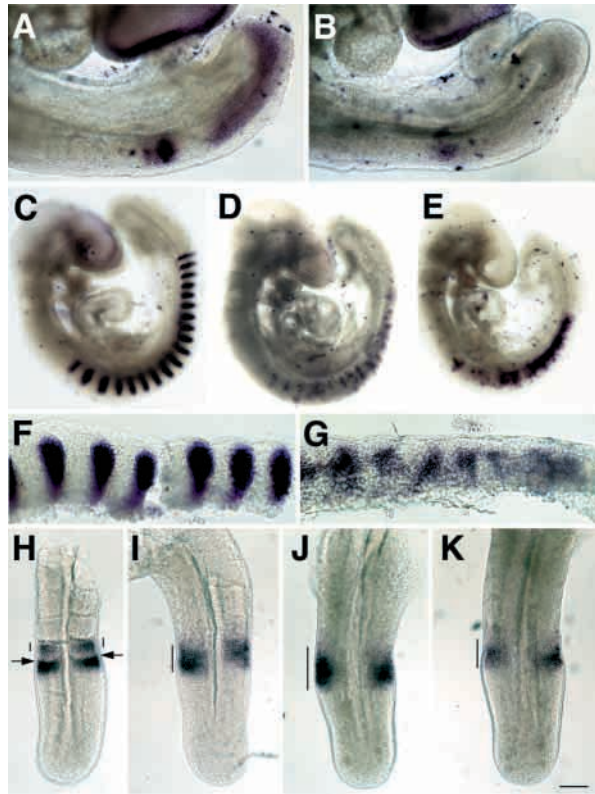
Fig. 6. The 'segmentation clock' and anteroposterior identity are disrupted in trunk paraxial mesoderm of *Dll3^neo/Dll3^neo* mutant embryos. (A-E) Lateral views. (A) At 9.5 dpc, *Lfng* expression is detected in two domains in the presomitic mesoderm of this *Dll3/Dll3^neo* embryo: rostrally, as one or two bands (the anteriormost is just caudal to the forming somite boundary); and caudally extending to the primitive streak. (B) *Lfng* expression is never detected caudally in the presomitc mesoderm of *Dll3^neo/Dll3^neo* embryos and rostral expression was diffuse. *Uncx4.1* expression shows clear periodicity in *Dll3/Dll3^neo* embryos at 9.5 dpc (C). (F) Expression is clearly restricted to the posterior of epithelial somites dissected from (C). (D,E) *Uncx4.1* expression is reduced in *Dll3^neo/Dll3^neo* mutants. Periodic expression is partially retained in some embryos (D) or lost (E). (G) Trunk paraxial mesoderm dissected from D; expression appears periodic but is not restricted to the posterior somite (note the lack of epithelial structure). Dorsal view showing *Cer1* expression in the tail region at 10.5 dpc of *Dll3/Dll3^neo* (H) and *Dll3^neo/Dll3^neo* embryos (I-K). (H) *Cer1* is expressed anteriorly in the presumptive somite and the nascent somite. Arrows mark the site of the most recently formed somite boundary and vertical bars show expression in the anterior of the nascent somite. (I-K) *Cer1* is expressed in a broad domain (vertical bar) as the bands of expression are missing. Scale bar: 125 μm in A,B; 300 μm in C-E; 60 μm in F,G; 120 μm (H-K).

Defining downstream effectors of *Dll3*-mediated Notch signalling

As *Hes5, Hes1* and *Hey1* have been identified as genes responsive to Notch signalling, their expression was examined in *Dll3^neo/Dll3^neo* embryos. *Hes5* is normally expressed as a band in rostral presomitic mesoderm in the posterior half of the forming somite (de la Pompa et al., 1997; del Barco Barrantes et al., 1999; Takebayashi et al., 1995). Analysis of gene expression at 10.5 dpc revealed four distinct patterns of
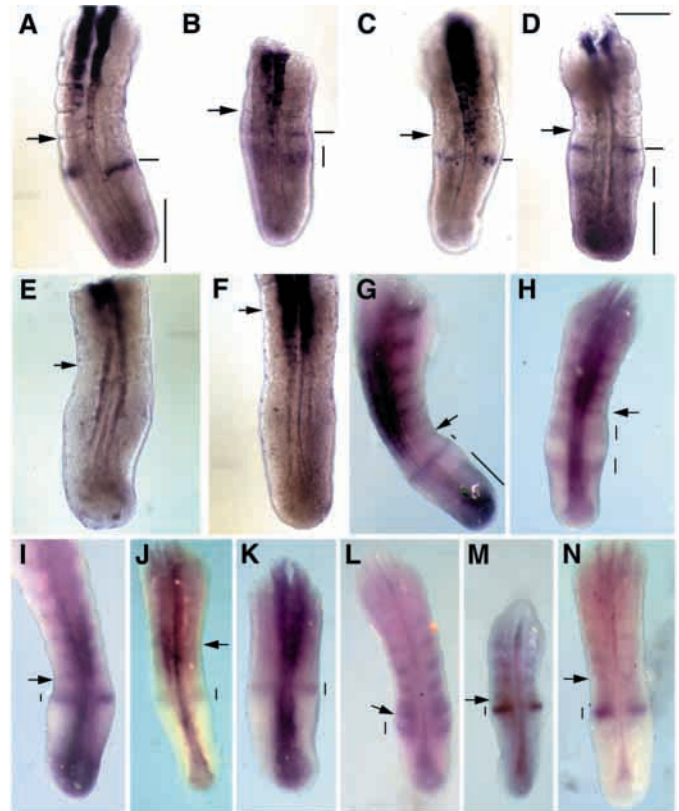
Fig. 7. *Hes5*, *Hes1* and *Hey1* expression is altered in *Dll3^neo/Dll3^neo* mutants. Gene expression determined by whole-mount RNA in situ hybridisation. Dorsal view of tail region from 10.5 dpc embryos, caudal boundary of most recently formed somite marked with an arrow. (A-F) *Hes5* expression; (A-D) four distinct patterns of *Hes5* expression identified in *Dll3/Dll3* and *Dll3/Dll3^neo* embryos. A tight band of *Hes5* expression is marked with a horizontal line; broader caudal domains of expression are marked with a vertical line. *Hes5* is also strongly expressed in the neural tube. (E,F) *Hes5* is not detected in the presomitic mesoderm of *Dll3^neo/Dll3^neo* mutants, despite being strongly detected in the neural tube. (G-I) Three distinct patterns of *Hes1* expression are detected in the presomitic mesoderm of *Dll3/Dll3* and *Dll3/Dll3^neo* embryos. Vertical lines indicate bands/domains of expression. *Hes1* expression is also detected in the caudal somite. (J,K) Only a single, relatively narrow band of *Hes1* expression is detected in the presomitic mesoderm of *Dll3^neo/Dll3^neo* mutant, this is located rostrally. Tail regions showing *Hes5* (A-D) and *Hes1* (G-I) expression are arranged in a hypothetical progression, according to the oscillatory expression of *Hes1* (Jouve et al., 2000). *Hey1* expression is clearly detected in the caudal somite in *Dll3/Dll3* and *Dll3/Dll3^neo* embryos (L,M) but not *Dll3^neo/Dll3^neo* mutants (N). Dynamic *Hey1* expression is represented in (L,M) with a broad band of expression in the presomitic mesoderm (vertical line, L) that condenses (vertical line, M) in *Dll3/Dll3* and *Dll3/Dll3^neo* embryos. Only a single narrow band of expression (vertical line) is detected in *Dll3^neo/Dll3^neo* mutants (N). Scale bar: 200 μm in A-F; 250 μm in G-K.

expression in presomitic mesoderm of *Dll3/Dll3* and *Dll3/Dll3^neo* embryos. These patterns of expression indicate that *Hes5*, like closely related *Hes1* and *Hes7*, is dynamically expressed in the presomitic mesoderm (Fig. 7A-D) (Bessho et al., 2001; Jouve et al., 2000). By contrast, at 10.5 dpc, *Hes5* expression was not detected in presomitic mesoderm in eight
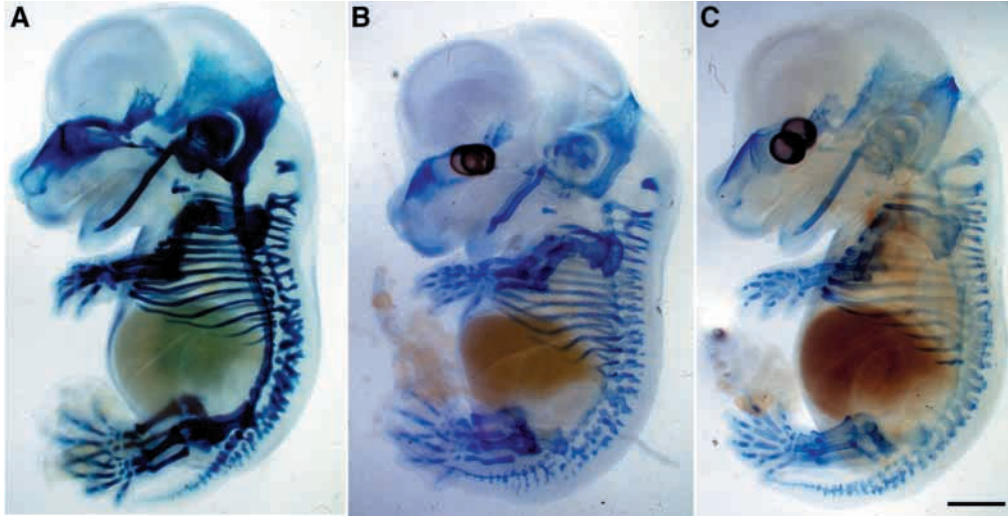
Fig. 8. *Dll3^{neo}* and *Dll3^{pu}* are equivalent alleles with respect to skeletal dysplasia. Lateral views of Alcian Blue-stained 14.5 dpc embryos. (A) *Dll3^{neo}/Dll3^{neo}*, (B) *Dll3^{neo}/Dll3^{pu}*, (C) *Dll3^{pu}/Dll3^{pu}*. The skeletal primordia appear to be in greater disarray and there are fewer coccygeal vertebrae in A than in C. Scale bar: 1.25 mm.

out of nine *Dll3^{neo}/Dll3^{neo}* mutant embryos (Fig. 7E,F). In one embryo, a single faint band was detected in rostral presomitic mesoderm (data not shown). Similarly, at 9.5 dpc, *Hes5* expression was not detected in presomitic mesoderm in six out of six *Dll3^{neo}/Dll3^{neo}* mutant embryos (data not shown). *Hes1* is expressed in the caudal half of nascent somites and dynamically in presomitic mesoderm (Jouve et al., 2000). In the presomitic mesoderm of *Dll3/Dll3* and *Dll3/Dll3^{neo}* embryos, dynamic expression is detected as a broad caudal domain that appears to narrow as it moves rostrally to form a tight band coincident with somite formation (Fig. 7G-I). Rostral expression is evident alone or in combination with this caudal domain of expression, depending upon the stage of the cycle. At 10.5 dpc *Dll3/Dll3* embryos exhibited either rostral alone (3/10) or rostral and caudal domains (7/10) of *Hes1* expression. Similarly *Hes1* expression was detected as a single rostral domain (6/11) or with rostral and caudal domains (5/11) in *Dll3/Dll3^{neo}*. This pattern of expression was not evident in *Dll3^{neo}/Dll3^{neo}* mutant embryos because, in ten out of ten, only a single narrow band of *Hes1* expression was detected in the rostral presomitic mesoderm (Fig. 7J,K). In addition, no *Hes1* expression was detected in the somites where normally it is detected caudally (compare Fig. 7G-I with 7J,K). *Hey1* is expressed in the caudal half of the most recently formed somite and in a band in the rostral presomitic mesoderm which narrows as a somite forms (Kokubo et al., 1999; Leimeister et al., 1999). *Hey1* expression in wild-type (*Dll3/Dll3*) and heterozygous (*Dll3/Dll3^{neo}*) embryos reflects this pattern of expression with 10/24 embryos the same as Fig. 7L and 14/24 the same as Fig. 7M. By contrast, in 18 out of 18 *Dll3^{neo}/Dll3^{neo}* mutant embryos, *Hey1* expression appeared static because only a single band of expression was detected in the rostral presomitic mesoderm (Fig. 7N). In addition, expression normally present in the caudal somites was not detectable in most mutants (compare Fig. 7L,M with 7N). In summary, these data demonstrate that *Dll3* is required for the normal expression of *Hes5, Hes1* and *Hey1* in presomitic mesoderm.

Dll3^{neo} and *Dll3^{pu}* are equivalent alleles with respect the generation of axial skeletal defects

Postnatal analysis of pudgy mice demonstrated that the *Dll3^{pu}* allele resulted in truncation of the body, misaligned vertebrae, rib fusions and a short tail in homozygous individuals (Gruneberg, 1961; Kusumi et al., 1998). We extended this analysis and observed at 14.5 dpc that defects in the preskeleton of *Dll3^{pu}/Dll3^{pu}* were very similar to those of *Dll3^{neo}/Dll3^{neo}* embryos. However, slight differences were evident such that the dysplasia of *Dll3^{pu}/Dll3^{pu}* embryos was less severe and the tail was longer. Genetic analysis revealed that the *Dll3^{neo}* and *Dll3^{pu}* alleles were equivalent with respect to the skeletal defects as preskeletons in *Dll3^{neo}/Dll3^{pu}*, *Dll3^{neo}/Dll3^{neo}* and *Dll3^{pu}/Dll3^{pu}* were similar (Fig. 8).

DISCUSSION

The mutant *Dll3* alleles; *Dll3^{neo}*, *Dll3^{pu}* and *DLL3-SCD* are functionally equivalent with respect to skeletal dysplasia

Uncertainty has surrounded the mouse *Dll3^{pu}* allele because it is unclear whether this allele is null. Although a four base deletion is predicted to generate a stop codon in exon 3 (N-terminal to the DSL that lies in exon 4) (Kusumi et al., 1998), it is possible that splicing around the deletion occurs and some functional *Dll3* protein is produced. As we have been unable to generate anti-Dll3 antibodies this scenario has remained untested; however, our genetic complementation studies indicate that this is unlikely to be the case because *Dll3^{neo}* and *Dll3^{pu}* are equivalent alleles with respect to skeletal dysplasia (Fig. 8). We observed that *Dll3^{neo}/Dll3^{neo}* individuals are slightly more severely affected than *Dll3^{pu}/Dll3^{pu}*, but this is likely to be due to differences in mouse strain (*Dll3^{neo}/Dll3^{neo}* embryos are 129Ola/C57BL6, whereas the *Dll3^{pu}/Dll3^{pu}* embryos are C3H/He/C57BL6). In humans, sequence analysis has defined three SCD-associated *DLL3* mutations. SD1 contains a five base insertion, SD2 a two base deletion and SD3 a missense mutation in EGF repeat number 5 (Bulman et al., 2000). The effect of the missense mutation on protein function is unknown; however, SD1 and SD2 mutations generate truncated proteins that are not membrane tethered but could interact with Notch because the DSL (Notch-binding region) is present either in full (SD2) or in part (SD1). This raises the possibility that these mutants do not represent null alleles,

because soluble DLL3 forms could interact with Notch and either activate the receptor without being tethered to a neighbouring cell or prevent another ligand from binding Notch. However, as the *Dll3^neo* null mutation has very similar phenotypic effects on the development of the axial skeleton, we suggest that each of the human SCD alleles are likely to represent null mutations.

The developmental origin of skeletal defects associated with SCD lie in the disruption of the segmentation clock within the presomitic mesoderm

Generation of the *Dll3^neo* mutant mouse lines has allowed us to examine the developmental origins of the skeletal defects presented in SCD. The core SCD phenotype is characterised by multiple hemi-vertebrae with rib fusions and deletions. The developmental origins of this phenotype reside in aberrant somite formation – a defect that appears grounded in the loss of the oscillatory mechanism that drives the regular periodicity with which somites are formed. The molecular analysis of *Dll3^neo/Dll3^neo* embryos identifies genes associated with Notch signalling, whose normal expression in the presomitic mesoderm is dependent upon *Dll3* function. These include *Lfng*, *Hes5*, *Hes1* and *Hey1*, and therefore these are candidate genes responsible for cases of SCD that show no link to *DLL3*/19q13.

Are Dll1 and Dll3 distinct ligands of Notch in paraxial mesoderm?

Both *Dll1* and *Dll3* are required for normal somite formation and correct specification of anteroposterior polarity within the presomitic mesoderm (Gruneberg, 1961; Hrabe de Angelis et al., 1997; Kusumi et al., 1998) (Figs 5, 6). As Dll1 and Dll3 are both ligands of Notch, what evidence is there that they are distinct ligands that elicit different downstream responses? This study shows that markers of anterior (*Cer1*) and posterior (*Uncx4.1*) somite identity are expressed at normal levels in the absence of *Dll3*, but that the periodic expression of *Uncx4.1* and *Cer1*, which is characteristic of anteroposterior polarity, is lost (Fig. 6 and summarised in Fig. 9). By contrast, anteroposterior identity is lost in *Dll1* mutants, as *Uncx4.1* is not detected, while *Cer1* (and *EphA4* another marker of anterior) are severely downregulated (del Barco Barrantes et al., 1999) (Fig. 9). In addition, we present evidence to suggest that Dll1 and Dll3 elicit distinct responses from genes associated with Notch signalling. For example, a loss-of-function mutation in *Dll1* results in severely downregulated (and largely undetected) expression of *Lfng*, *Hes5*, *Hes1*, *Hey1*, *Mesp1* and *Mesp2* in presomitic mesoderm (del Barco Barrantes et al., 1999; Jouve et al., 2000; Kokubo et al., 1999) (Fig. 9). By contrast, with the exception of *Hes5*, the expression of each of these genes is readily detected in presomitic mesoderm of *Dll3* null mutants (Figs 5-7, 9; *Mesp1* was not examined). That Dll1 and Dll3 may be distinct is further supported by the fact that Dll3 is a highly divergent Delta homologue (Dunwoodie et al., 1997) and has only 18% identity to the Notch binding DSL of Dll1, compared with the 51% identity between Dll4 and Dll1. It is, however, possible that when *Dll1* and *Dll3* mutants are compared that some of the observed differences in gene expression do not indicate discrete functions for these ligands but rather reflect the possibility that *Dll1* and *Dll3* perform the same function and
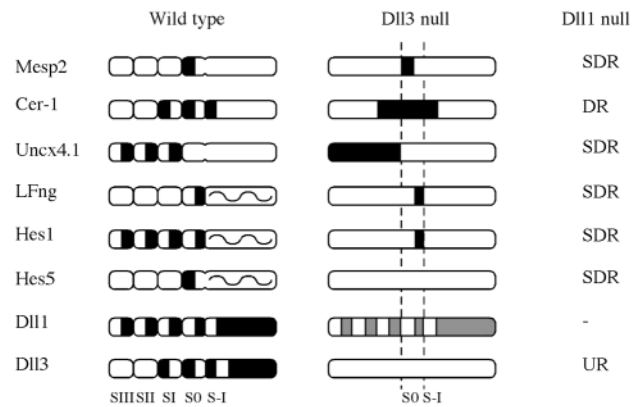
Fig. 9. A comparison of gene expression in paraxial mesoderm of normal and Delta mutants. Black and grey areas represent localisation of transcript and the wavy line represents dynamic gene expression. The most recently formed somite is SI, the forming somite is S0, and the block of presomitic mesoderm cells of one somite length (caudal to S0) is S-I according to (Dale and Pourquie, 2000; Ordahl, 1993). Gene expression was determined by RNA in situ hybridisation. This study examined expression in wild-type and *Dll3* mutant embryos. Wild-type expression patterns were in accordance with those previously reported: *Mesp2* (Saga et al., 1996), *Cer1* (Biben et al., 1998), *Uncx4.1* (Mansouri et al., 1997; Neidhardt, 1997), *Lfng* (Forsberg et al., 1998; Johnston et al., 1997), *Hes1* (Jouve et al., 2000), *Dll1* (Bettenhausen et al., 1995; Dunwoodie et al., 1997) and *Dll3* (Dunwoodie et al., 1997). For *Hes5*, we identified four distinct patterns of expression in presomitic mesoderm (Fig. 7). Gene expression in *Dll1* mutants is based on previous reports (del Barco Barrantes et al., 1999; Jouve et al., 2000). The levels of expression of *Dll1* in *Dll3* mutant embryos was low with diffuse boundaries and is indicated by grey shading.

affect the expression of specific genes to different extents. As *Dll1* and *Dll3* are differentially expressed in presumptive and nascent somites, this issue could best be addressed by placing the *Dll1* cDNA under the regulatory control of *Dll3* or vice versa using a cDNA 'knock-in' approach.

Oscillatory gene expression in the presomitic mesoderm

Genes expressed in an oscillatory manner in the presomitic mesoderm are likely to hold the key to our understanding of how exactly Notch signalling controls somitogenesis. We show for the first time that *Hes5* exhibits a number of distinct patterns of expression in the presomitic mesoderm. This suggests that *Hes5*, like *Hes1* and *Hes7*, is expressed under the control of oscillatory stimuli. The regulatory parameters that control the dynamic expression of these 'clock' genes in presomitic mesoderm are unknown. We present data to indicate that the rostral and caudal expression components of these genes are differentially controlled by Dll3 and Dll1. Expression of *Lfng* is severely downregulated (del Barco Barrantes et al., 1999) and *Hes1* is not detected (Jouve et al., 2000) in the presomitic mesoderm of *Dll1* null mutants, but in *Dll3^neo* null mutants, only the caudal expression component is lost with the rostral band clearly evident (Figs 6, 7, 9). These differences could simply be due to different levels of gene expression; however, this does not appear to be the case because the rostral and caudal expression domains of *Hes1* in

the presomitic mesoderm normally occur at equal levels and so the loss of just the caudal domain in *Dll3* mutants cannot be explained by an overall reduction in expression levels. In the case of *Lfng*, even though the rostral domain is normally expressed at levels higher than that seen caudally, rostral expression in *Dll3* mutants was readily detectable and no caudal expression was ever observed, even under extensive periods of staining. This suggests that the rostral and caudal components that drive expression of oscillatory genes such as *Hes1* and *Lfng* in the presomitic mesoderm are independently controlled and that both components require Dll1, but only the caudal component requires Dll3.

A comparison of Dll3 and deltaD mutants

The mutant phenotype of *Dll3* resembles that of *deltaD* (*after eight*) in zebrafish at a number of levels. First, in both mutants somite formation occurs in the first instance with what appears to be the correct periodicity. This is followed by delayed somite formation in *Dll3* mutants, and lack of somite formation in *deltaD* mutants. However, even though metamerism was apparent in *Dll3* mutants, borders between somites were not evident and condensation of paraxial mesoderm into somites was reduced compared with wild type (Fig. 5). That somitogenesis is not completely normal is supported by the fact that the vertebra caudal to and including cervical 1 (which is comprised of the anterior part of the fifth formed somite) was not properly formed. Second, marker gene expression indicates that paraxial mesoderm in *Dll3* and *deltaD* mutants has both anterior (*Dll3 – Cer1* and *Mesp2*; *deltaD – mesp-a*, *EphA4*, *fgf8* and *deltaD*) and posterior (*Dll3 – Uncx4.1* and *Cited1*; *deltaD – ephrin-B2* and *MyoD*) character (Fig. 6, data not shown) (Durbin et al., 2000). Third, although paraxial mesoderm has anterior and posterior identity in both mutants, like cells are not grouped and spaced periodically (Fig. 6) (Durbin et al., 2000). Finally, both mutants show disrupted expression of genes expressed in a cyclical manner in the presomitic mesoderm. In *Dll3* mutants, *Lfng*, *Hes1* and *Hes5* expression is disrupted, while in *deltaD*, *her1* expression is disrupted. As mutant expression of *Lfng*, *Hes1* and *her1* consists of what appears to be a static band in the rostral presomitic mesoderm in the absence of caudal expression, there is potentially a common mechanism that is responsible for the oscillatory gene expression in presomitic mesoderm (Fig. 7) (Holley et al., 2000).

REFERENCES

Akazawa, C., Sasai, Y., Nakanishi, S. and Kageyama, R. (1992). Molecular characterization of a rat negative regulator with a basic helix-loop-helix structure predominantly expressed in the developing nervous system. *J. Biol. Chem.* **267**, 21879-21885.

Artavanis-Tsakonas, S., Rand, M. D. and Lake, R. J. (1999). Notch signaling: cell fate control and signal integration in development. *Science* **284**, 770-776.

Aulehla, A. and Johnson, R. L. (1999). Dynamic expression of lunatic fringe suggests a link between notch signaling and an autonomous cellular oscillator driving somite segmentation. *Dev. Biol.* **207**, 49-61.

Bagnall, K. M., Higgins, S. J. and Sanders, E. J. (1988). The contribution made by a single somite to the vertebral column: experimental evidence in support of resegmentation using the chick- quail chimaera model. *Development* **103**, 69-85.

Bagnall, K. M., Higgins, S. J. and Sanders, E. J. (1989). The contribution made by cells from a single somite to tissues within a body segment and assessment of their integration with similar cells from adjacent segments. *Development* **107**, 931-943.

Bailey, A. M. and Posakony, J. W. (1995). Suppressor of hairless directly activates transcription of enhancer of split complex genes in response to Notch receptor activity. *Genes Dev.* **9**, 2609-2622.

Bessho, Y., Miyoshi, G., Sakata, R. and Kageyama, R. (2001). Hes7: a bHLH-type repressor gene regulated by Notch and expressed in the presomitic mesoderm. *Genes Cells* **6**, 175-185.

Bettenhausen, B., Hrabe de Angelis, M., Simon, D., Guenet, J. L. and Gossler, A. (1995). Transient and restricted expression during mouse embryogenesis of Dll1, a murine gene closely related to Drosophila Delta. *Development* **121**, 2407-2418.

Biben, C., Stanley, E., Fabri, L., Kotecha, S., Rhinn, M., Drinkwater, C., Lah, M., Wang, C. C., Nash, A., Hilton, D. et al. (1998). Murine cerberus homologue mCer-1: a candidate anterior patterning molecule. *Dev. Biol.* **194**, 135-151.

Bray, S. (1998). Notch signalling in Drosophila: three ways to use a pathway. *Semin. Cell Dev. Biol.* **9**, 591-597.

Bronner Fraser, M. (1986). Analysis of the early stages of trunk neural crest migration in avian embryos using monoclonal antibody HNK-1. *Dev. Biol.* **155**, 44-55.

Bulman, M. P., Kusumi, K., Frayling, T. M., McKeown, C., Garrett, C., Lander, E. S., Krumlauf, R., Hattersley, A. T., Ellard, S. and Turnpenny, P. D. (2000). Mutations in the human delta homologue, DLL3, cause axial skeletal defects in spondylocostal dysostosis. *Nat. Genet.* **24**, 438-441.

Conlon, R. A., Reaume, A. G. and Rossant, J. (1995). Notch1 is required for the coordinate segmentation of somites. *Development* **121**, 1533-1545.

Cooke, J. and Zeeman, E. C. (1976). A clock and wavefront model for control of the number of repeated structures during animal morphogenesis. *J. Theor. Biol.* **58**, 455-476.

Cooke, J. (1998). A gene that resuscitates a theory–somitogenesis and a molecular oscillator. *Trends Genet.* **14**, 85-88.

Dale, K. J. and Pourquie, O. (2000). A clock-work somite. *BioEssays* **22**, 72-83.

de Celis, J. F. and Bray, S. (1997). Feed-back mechanisms affecting Notch activation at the dorsoventral boundary in the Drosophila wing. *Development* **124**, 3241-3251.

de la Pompa, J. L., Wakeham, A., Correia, K. M., Samper, E., Brown, S., Aguilera, R. J., Nakano, T., Honjo, T., Mak, T. W., Rossant, J. et al. (1997). Conservation of the Notch signalling pathway in mammalian neurogenesis. *Development* **124**, 1139-1148.

del Barco Barrantes, I., Elia, A. J., Wunsch, K., De Angelis, M. H., Mak, T. W., Rossant, J., Conlon, R. A., Gossler, A. and de la Pompa, J. L. (1999). Interaction between Notch signalling and Lunatic fringe during somite boundary formation in the mouse. *Curr. Biol.* **9**, 470-480.

Dunwoodie, S. L., Henrique, D., Harrison, S. M. and Beddington, R. S. (1997). Mouse Dll3: a novel divergent Delta gene which may complement the function of other Delta homologues during early pattern formation in the mouse embryo. *Development* **124**, 3065-3076.

Durbin, L., Sordino, P., Barrios, A., Gering, M., Thisse, C., Thisse, B., Brennan, C., Green, A., Wilson, S. and Holder, N. (2000). Anteroposterior patterning is required within segments for somite boundary formation in developing zebrafish. *Development* **127**, 1703-1713.

Egan, S. E., St-Pierre, B. and Leow, C. C. (1998). Notch receptors, partners and regulators: from conserved domains to powerful functions. *Curr. Top. Microbiol. Immunol.* **228**, 273-324.

Evrard, Y. A., Lun, Y., Aulehla, A., Gan, L. and Johnson, R. L. (1998). lunatic fringe is an essential mediator of somite segmentation and patterning. *Nature* **394**, 377-381.

Fleming, R. J., Scottgale, T. N., Diederich, R. J. and Artavanis-Tsakonas, S. (1990). The gene Serrate encodes a putative EGF-like transmembrane protein essential for proper ectodermal development in Drosophila melanogaster. *Genes Dev.* **4**, 2188-2201.

Fleming, R. J., Gu, Y. and Hukriede, N. A. (1997). Serrate-mediated activation of Notch is specifically blocked by the product of the gene fringe

in the dorsal compartment of the Drosophila wing imaginal disc. *Development* **124**, 2973-2981.

Forsberg, H., Crozet, F. and Brown, N. A. (1998). Waves of mouse Lunatic fringe expression, in four-hour cycles at two-hour intervals, precede somite boundary formation. *Curr. Biol.* **8**, 1027-1030.

Furukawa, T., Maruyama, S., Kawaichi, M. and Honjo, T. (1992). The Drosophila homolog of the immunoglobulin recombination signal- binding protein regulates peripheral nervous system development. *Cell* **69**, 1191-1197.

Goedbloed, J. F. and Smits-van Prooije, A. E. (1986). Quantitative analysis of the temporal pattern of somite formation in the mouse and rat. A simple and accurate method for age determination. *Acta Anat.* **125**, 76-82.

Greenwald, I. (1998). LIN-12/Notch signaling: lessons from worms and flies. *Genes Dev.* **12**, 1751-1762.

Gruneberg, H. (1961). Genetical studies on the skeleton of the mouse XXIX Pudgy. *Genetic Res.* **2**, 384-393.

Harrison, S. M., Dunwoodie, S. L., Arkell, R. M., Lehrach, H. and Beddington, R. S. (1995). Isolation of novel tissue-specific genes from cDNA libraries representing the individual tissue constituents of the gastrulating mouse embryo. *Development* **121**, 2479-2489.

Heitzler, P. and Simpson, P. (1991). The choice of cell fate in the epidermis of Drosophila. *Cell* **64**, 1083-1092.

Hogan, B., Beddington, R., Costantini, F. and Lacy, E. (1994). *Manipulating the Mouse Embryo. A Laboratory Manual*. New York: Cold Spring Harbor Laboratory Press.

Holley, S. A., Geisler, R. and Nusslein-Volhard, C. (2000). Control of her1 expression during zebrafish somitogenesis by a delta- dependent oscillator and an independent wave-front activity. *Genes Dev.* **14**, 1678-1690.

Hrabe de Angelis, M., McIntyre, J., 2nd and Gossler, A. (1997). Maintenance of somite borders in mice requires the Delta homologue DlI1. *Nature* **386**, 717-721.

Huang, R., Zhi, Q., Neubuser, A., Muller, T. S., Brand-Saberi, B., Christ, B. and Wilting, J. (1996). Function of somite and somitocoele cells in the formation of the vertebral motion segment in avian embryos. *Acta Anat.* **155**, 231-241.

Huppert, S. S., Jacobsen, T. L. and Muskavitch, M. A. (1997). Feedback regulation is central to Delta-Notch signalling required for Drosophila wing vein morphogenesis. *Development* **124**, 3283-3291.

Jegalian, B. G. and De Robertis, E. M. (1992). Homeotic transformations in the mouse induced by overexpression of a human Hox3.3 transgene. *Cell* **71**, 901-910.

Jiang, Y.-J., Aerne, B. L., Smithers, L., Haddon, C., Ish-Horowicz, D. and Lewis, J. (2000). Notch signalling and the synchronization of the somite segmentation clock. *Nature* **408**, 475-479.

Johnston, S. H., Rauskolb, C., Wilson, R., Prabhakaran, B., Irvine, K. D. and Vogt, T. F. (1997). A family of mammalian Fringe genes implicated in boundary determination and the Notch pathway. *Development* **124**, 2245-2254.

Jouve, C., Palmeirim, I., Henrique, D., Beckers, J., Gossler, A., Ish-Horowicz, D. and Pourquie, O. (2000). Notch signalling is required for cyclic expression of the hairy-like gene HES1 in the presomitic mesoderm. *Development* **127**, 1421-1429.

Kaufman, M. H. (1992). *The Atlas of Mouse Development*. London: Academic Press.

Kimble, J. and Simpson, P. (1997). The LIN-12/Notch signaling pathway and its regulation. *Annu. Rev. Cell Dev. Biol.* **13**, 333-361.

Klein, T. and Arias, A. M. (1998). Interactions among Delta, Serrate and Fringe modulate Notch activity during Drosophila wing development. *Development* **125**, 2951-2962.

Kokubo, H., Lun, Y. and Johnson, R. L. (1999). Identification and expression of a novel family of bHLH cDNAs related to Drosophila hairy and enhancer of split. *Biochem. Biophys. Res. Commun.* **260**, 459-465.

Krantz, I. D., Piccoli, D. A. and Spinner, N. B. (1997). Alagille syndrome. *J. Med. Genet.* **34**, 152-157.

Kusumi, K., Sun, E. S., Kerrebrock, A. W., Bronson, R. T., Chi, D. C., Bulotsky, M. S., Spencer, J. B., Birren, B. W., Frankel, W. N. and Lander, E. S. (1998). The mouse pudgy mutation disrupts Delta homologue Dll3 and initiation of early somite boundaries. *Nat. Genet.* **19**, 274-278.

Lardelli, M., Dahlstrand, J. and Lendahl, U. (1994). The novel Notch homologue mouse Notch 3 lacks specific epidermal growth factor-repeats and is expressed in proliferating neuroepithelium. *Mech. Dev.* **46**, 123-136.

Larsen, W. J. (1997). Development of the peripheral nervous system. In *Human Embryology*. pp. 107-125. New York: Churchill Livingstone.

Lecourtois, M. and Schweisguth, F. (1995). The neurogenic suppressor of hairless DNA-binding protein mediates the transcriptional activation of the enhancer of split complex genes triggered by Notch signaling. *Genes Dev.* **9**, 2598-2608.

Leimeister, C., Externbrink, A., Klamt, B. and Gessler, M. (1999). Hey genes: a novel subfamily of hairy- and Enhancer of split related genes specifically expressed during mouse embryogenesis. *Mech. Dev.* **85**, 173-177.

Leimeister, C., Dale, K., Fischer, A., Klamt, B., Hrabe de Angelis, M., Radtke, F., McGrew, M. J., Pourquie, O. and Gessler, M. (2000). Oscillating expression of c-hey2 in the presomitic mesoderm suggests that the segmentation clock may use combinatorial signaling through multiple interacting bHLH factors. *Dev. Biol.* **227**, 91-103.

Lindsell, C. E., Shawber, C. J., Boulter, J. and Weinmaster, G. (1995). Jagged: a mammalian ligand that activates Notch1. *Cell* **80**, 909-917.

Mansouri, A., Yokota, Y., Wehr, R., Copeland, N. G., Jenkins, N. A. and Gruss, P. (1997). Paired-related murine homeobox gene expressed in the developing sclerotome, kidney, and nervous system. *Dev. Dyn.* **210**, 53-65.

Mark, M., Lufkin, T., Vonesch, J. L., Ruberte, E., Olivo, J. C., Dolle, P., Gorry, P., Lumsden, A. and Chambon, P. (1993). Two rhombomeres are altered in Hoxa-1 mutant mice. *Development* **119**, 319-338.

McGrew, M. J., Dale, J. K., Fraboulet, S. and Pourquie, O. (1998). The lunatic fringe gene is a target of the molecular clock linked to somite segmentation in avian embryos. *Curr. Biol.* **8**, 979-982.

Mitsiadis, T. A., Henrique, D., Thesleff, I. and Lendahl, U. (1997). Mouse Serrate-1 (Jagged-1): expression in the developing tooth is regulated by epithelial-mesenchymal interactions and fibroblast growth factor-4. *Development* **124**, 1473-1483.

Nakagawa, O., Nakagawa, M., Richardson, J. A., Olson, E. N. and Srivastava, D. (1999). HRT1, HRT2, and HRT3: a new subclass of bHLH transcription factors marking specific cardiac, somitic, and pharyngeal arch segments. *Dev. Biol.* **216**, 72-84.

Neidhardt, L. M., Kispert, A. and Herrmann, B. G. (1997). A mouse gene of the paired-related homeobox class expressed in the caudal somite compartment and in the developing vertebral column, kidney and nervous system. *Dev. Genes Evol.* **207**, 330-339.

Ohtsuka, T., Ishibashi, M., Gradwohl, G., Nakanishi, S., Guillemot, F. and Kageyama, R. (1999). Hes1 and Hes5 as notch effectors in mammalian neuronal differentiation. *EMBO J.* **18**, 2196-2207.

Oka, C., Nakano, T., Wakeham, A., de la Pompa, J. L., Mori, C., Sakai, T., Okazaki, S., Kawaichi, M., Shiota, K., Mak, T. W. and Honjo, T. (1995). Disruption of the mouse RBP-J kappa gene results in early embryonic death. *Development* **121**, 3291-3301.

Ordahl, C. (1993). In *Myogenic Lineages within the Developing Somite* (ed. M. Bernfield), pp. 165-176. New York: John Wiley and Sons.

Palmeirim, I., Henrique, D., Ish-Horowicz, D. and Pourquie, O. (1997). Avian hairy gene expression identifies a molecular clock linked to vertebrate segmentation and somitogenesis. *Cell* **91**, 639-648.

Panin, V. M., Papayannopoulos, V., Wilson, R. and Irvine, K. D. (1997). Fringe modulates Notch-ligand interactions. *Nature* **387**, 908-912.

Pourquie, O. (2000). Vertebrate segmentation: is cycling the rule? *Curr. Opin. Cell Biol.* **12**, 747-751.

Rickmann, M., Fawcett, J. W. and Keynes, R. J. (1985). The migration of neural crest cells and the growth of motor axons through the rostral half of the chick somite. *J. Embryol. Exp. Morphol.* **90**, 437-455.

Saga, Y., Hata, N., Kobayashi, S., Magnuson, T., Seldin, M. F. and Taketo, M. M. (1996). MesP1: a novel basic helix-loop-helix protein expressed in the nascent mesodermal cells during mouse gastrulation. *Development* **122**, 2769-2778.

Saga, Y., Hata, N., Koseki, H. and Taketo, M. M. (1997). Mesp2: a novel mouse gene expressed in the presegmented mesoderm and essential for segmentation initiation. *Genes Dev.* **11**, 1827-1839.

Sasai, Y., Kageyama, R., Tagawa, Y., Shigemoto, R. and Nakanishi, S. (1992). Two mammalian helix-loop-helix factors structurally related to Drosophila hairy and Enhancer of split. *Genes Dev.* **6**, 2620-2634.

Schweisguth, F. and Posakony, J. W. (1992). Suppressor of Hairless, the Drosophila homolog of the mouse recombination signal-binding protein gene, controls sensory organ cell fates. *Cell* **69**, 1199-1212.

Shawber, C., Boulter, J., Lindsell, C. E. and Weinmaster, G. (1996). Jagged2: a serrate-like gene expressed during rat embryogenesis. *Dev. Biol.* **180**, 370-376.

Shutter, J. R., Scully, S., Fan, W., Richards, W. G., Kitajewski, J., Deblandre, G. A., Kintner, C. R. and Stark, K. L. (2000). Dll4, a novel Notch ligand expressed in arterial endothelium. *Genes Dev.* **14**, 1313-1318.

Stern, C. D. and Keynes, R. J. (1987). Interactions between somite cells: the

formation and maintenance of segment boundaries in the chick embryo. *Development* **99**, 261-272.

Swiatek, P. J., Lindsell, C. E., del Amo, F. F., Weinmaster, G. and Gridley, T. (1994). Notch1 is essential for postimplantation development in mice. *Genes Dev.* **8**, 707-719.

Takebayashi, K., Akazawa, C., Nakanishi, S. and Kageyama, R. (1995). Structure and promoter analysis of the gene encoding the mouse helix- loop-helix factor HES-5. Identification of the neural precursor cell- specific promoter element. *J. Biol. Chem.* **270**, 1342-1349.

Tam, P. P. and Tan, S. S. (1992). The somitogenetic potential of cells in the primitive streak and the tail bud of the organogenesis-stage mouse embryo. *Development* **115**, 703-715.

Teillet, M. A., Kalcheim, C. and Le Douarin, N. M. (1987). Formation of the dorsal root ganglia in the avian embryo: segmental origin and migratory behavior of neural crest progenitor cells. *Dev. Biol.* **120**, 329-347.

Tosney, K. W. (1978). The early migration of neural crest cells in the trunk region of the avian embryo: An electron microscopic study. *Dev. Biol.* **62**, 317-333.

Uyttendaele, H., Marazzi, G., Wu, G., Yan, Q., Sassoon, D. and Kitajewski, J. (1996). Notch4/int-3, a mammary proto-oncogene, is an endothelial cell-specific mammalian Notch gene. *Development* **122**, 2251-2259.

Vassin, H., Bremer, K. A., Knust, E. and Campos-Ortega, J. A. (1987). The neurogenic gene *Delta* of *Drosophila melanogaster* is expressed in neurogenic territories and encodes a putative transmembrane protein with EGF-like repeats. *EMBO J.* **6**, 3431-3440.

Weinmaster, G., Roberts, V. J. and Lemke, G. (1991). A homolog of Drosophila Notch expressed during mammalian development. *Development* **113**, 199-205.

Weinmaster, G., Roberts, V. J. and Lemke, G. (1992). Notch2: a second mammalian Notch gene. *Development* **116**, 931-941.

Weston, J. A. (1963). An radioautographic analysis of the migration and localization of trunk neural crest cells in the chick. *Dev. Biol.* **6**, 279-310.

Wharton, K. A., Johansen, K. M., Xu, T. and Artavanis-Tsakonas, S. (1985). Nucleotide sequence from the neurogenic locus notch implies a gene product that shares homology with proteins containing EGF-like repeats. *Cell* **43**, 567-581.

Wong, P. C., Zheng, H., Chen, H., Becher, M. W., Sirinathsinghji, D. J., Trumbauer, M. E., Chen, H. Y., Price, D. L., Van der Ploeg, L. H. and Sisodia, S. S. (1997). Presenilin 1 is required for Notch1 and DII1 expression in the paraxial mesoderm. *Nature* **387**, 288-292.

Xue, Y., Gao, X., Lindsell, C. E., Norton, C. R., Chang, B., Hicks, C., Gendron-Maguire, M., Rand, E. B., Weinmaster, G. and Gridley, T. (1999). Embryonic lethality and vascular defects in mice lacking the Notch ligand Jagged1. *Hum. Mol. Genet.* **8**, 723-730.

Zhang, N. and Gridley, T. (1998). Defects in somite formation in lunatic fringe-deficient mice. *Nature* **394**, 374-377.